

Polyion Complex Micelles Possessing Thermoresponsive Coronas and Their Covalent Core Stabilization via “Click” Chemistry

Jingyan Zhang,^{†,‡} Yueming Zhou,[‡] Zhiyuan Zhu,[‡] Zhishen Ge,[‡] and Shiyong Liu^{*‡}

School of Materials and Chemical Engineering, Anhui University of Architecture, Hefei, Anhui 230022, China, and Joint Laboratory of Polymer Thin Films and Solution, Department of Polymer Science and Engineering, Hefei National Laboratory for Physical Sciences at the Microscale, University of Science and Technology of China, Hefei, Anhui 230026, China

Received October 2, 2007; Revised Manuscript Received December 10, 2007

ABSTRACT: Two oppositely charged graft ionomers, P(MAA-co-AzPMA)-g-PNIPAM and P(QDMA-co-AzPMA)-g-PNIPAM, containing thermosensitive PNIPAM graft chains were successfully synthesized via a combination of atom transfer radical polymerization (ATRP) and “click” reactions, where PAzPMA, PMAA, PNIPAM, and PQDMA are poly(3-azidopropyl methacrylate), poly(methacrylic acid), poly(*N*-isopropylacrylamide), and poly(2-(dimethylamino)ethyl methacrylate) (PDMA) fully quaternized with methyl iodide, respectively. In aqueous solution, polyelectrolyte complexation between negatively charged backbone of P(MAA-co-AzPMA)-g-PNIPAM and positively charged backbone of P(QDMA-co-AzPMA)-g-PNIPAM leads to the formation of polyion complex (PIC) micelles consisting of polyion complex cores and thermoresponsive PNIPAM coronas. Upon addition of a difunctional cross-linker, propargy ether, PIC micelles can be facily cross-linked via “click” reactions. The obtained covalently core-stabilized PIC micelles exhibit permanent stability against the addition of NaCl and pH changes, which are drastically different from that of non-cross-linked PIC micelles. Moreover, these novel types of stable PIC micelles exhibit thermoinduced dispersion/aggregation due to the presence of PNIPAM coronas, suggesting that their physical affinity to external substrates can be tuned with temperature. They might act as stable nanocarriers of charged compounds or highly efficient nanoreactors of polar compounds in the field of pharmaceutical formulation or biotechnology.

Introduction

In aqueous solution, double hydrophilic block copolymers (DHBCs) can self-assemble into mesophases with varying morphologies such as micelles and vesicles, upon selectively rendering one of the blocks water-insoluble under proper external stimuli such as pH, temperature, ionic strength, light irradiation, and electric field.^{1–10} Polyelectrolyte complexation between two oppositely charged blocks can also be utilized to actuate the self-assembly of block copolymers, taking advantage of the fact that polyion complex (PIC) is insoluble at charge neutralization and can thus provide an alternate driving force for the micellization of neutral-polyelectrolyte block copolymers.^{11–21}

Original examples were reported by Kataoka et al.¹⁴ and Kabanov et al.¹⁵ in 1995, employing two oppositely charged neutral-polyelectrolyte block copolymers. In aqueous solution, the polyelectrolyte complexation between complementary blocks results in the formation of PIC micelles. Following this principle, various charged species such as ions, proteins, and nucleic acids can be encapsulated within the PIC micelle cores. Thus, ever-increasing attention has been paid to this research area due to their potential applications as delivery systems of protein drugs or therapeutic DNA. The presence of water-soluble neutral coronas can endow PIC micelles with enhanced chemical and structural stability during circulation, as compared to polyelectrolyte complexes prepared from protein or DNA and cationic liposomes or homopolyocations.^{15,22,23} On the other hand, the polar PIC micelle cores can act as segregated nanoreactors for

certain chemical reactions such as reduction of metal ions.^{18,24–26} It should be noted that the neutral water-soluble coronas, such as poly(ethylene oxide) (PEO), can also be replaced with stimuli-responsive ones, such as thermoresponsive poly(2-isopropyl-2-oxazoline), leading to the formation of environmentally sensitive PIC micelles for site-specific drug nanocarriers due to tunable affinity of substance affinity.^{27,28}

However, the above practical applications of PIC micelles are usually associated with large dilution (e.g., blood circulation after administration) and/or the presence of high concentration of salts. It has been well-proved that both cases might disintegrate PIC micelles. They will dissociate into unimer chains when the concentration falls below the critical micelle concentration (cmc). The presence of salts can screen electrostatic interactions between oppositely charged blocks and can eventually lead to the decomposition of PIC micelles.²⁹ Similar to those methodologies employed for the covalent stabilization of block copolymer micelles, such as shell cross-linking (SCL) or core cross-linking (CCL), PIC micelles can also be covalently stabilized to enhance their structural stability against changes of external conditions.^{24,29–33}

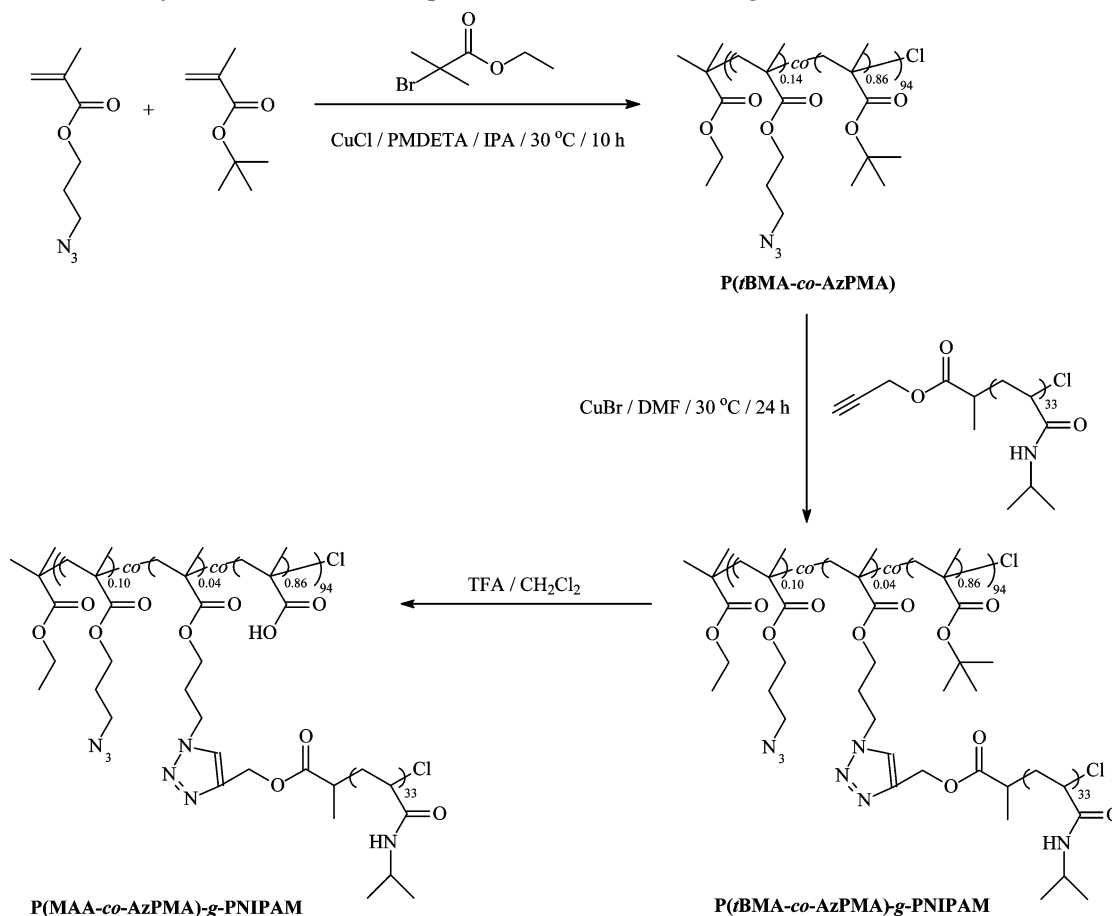
Kataoka et al.²⁹ prepared PIC micelles from poly(α,β -aspartic acid) (PAsp) and poly(ethylene oxide)-*b*-poly(L-lysine) (PEO-*b*-PLys) with PLys block being derivatized with thiol groups. The subsequent reversible core stabilization and dissociation can be achieved via the well-controlled formation and breakage of disulfide bonds via oxidation and the addition of excess of small molecule thiol compounds such as dithiothreitol (DTT). They also reported the stabilization of PIC micelles of PEO-*b*-PAsp and trypsin via the Schiff base formation upon addition of a difunctional reagent, glutaraldehyde.²⁴ Bronich and co-workers also reported that PIC micelles formed from poly(ethylene oxide)-*b*-poly(sodium methacrylate) (PEO-*b*-PNaMA)

* To whom correspondence should be addressed. E-mail: sliu@ustc.edu.cn.

[†] Anhui University of Architecture.

[‡] University of Science and Technology of China.

Scheme 1. Synthetic Routes for the Preparation of P(MAA-co-AzPMA)-g-PNIPAM Anionic Graft Ionomer



in the presence of CaCl_2 can also be covalently stabilized via reaction with 1,2-ethylenediamine.³⁰

Recently, “click” chemistry has been proved to be a highly efficient and quantitative reaction for the formation of stable covalent linkages between azido and alkyne groups in the presence of copper(I) catalysts.^{34–38} Just recently, Wooley et al.³⁹ reported the “click” core cross-linking of micelles self-assembled from amphiphilic polystyrene-*b*-poly(acrylic acid) (PS-*b*-PAA) block copolymer with the PS block employing alkyne residues in the presence of dendrimers surface-functionalized with azide moieties as cross-linking agents.

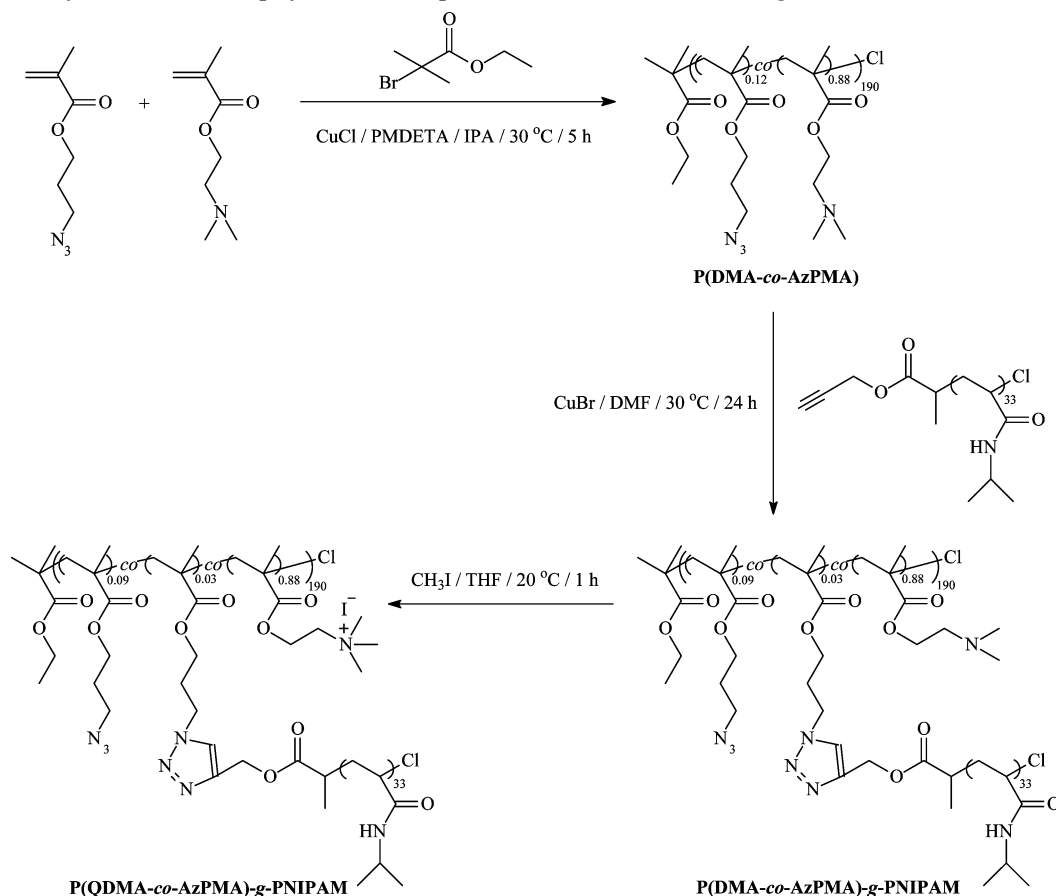
In the current investigation, we utilized “click” reactions for the covalent stabilization of PIC micelles. Recently, Matyjaszewski et al.³⁶ and Sumerlin et al.³⁷ reported that azide moieties are compatible with controlled radical polymerizations (CRPs) such as reversible addition–fragmentation chain transfer polymerization (RAFT) or atom transfer radical polymerization (ATRP), whereas the CRP of alkyne-containing monomers typically results in extensive gelation.³⁸ Thus, azide-containing monomer was incorporated into two oppositely charged backbones of two graft ionomers bearing well-known thermoresponsive poly(*N*-isopropylacrylamide) (PNIPAM)⁴⁰ graft chains (Schemes 1 and 2). The self-assembled PIC micelles in aqueous solution were subsequently core-stabilized via “click” reactions upon addition of a difunctional reagent, propargyl ether. The structural stability and thermosensitive aggregation of non-cross-linked and cross-linked PIC micelles were thoroughly characterized by laser light scattering (LLS) and temperature-dependent turbidimetry. To the best of our knowledge, the current study represents the first example of “click” stabilization of PIC micelles with thermosensitive coronas.

Experimental Section

Materials. *N*-Isopropylacrylamide (NIPAM, 97%, Tokyo Kasei Kagyo Co.) was purified by recrystallization from a mixture of benzene and *n*-hexane (1/3, v/v). *tert*-Butyl methacrylate (*t*BMA, 98%, TCI) and 2-(dimethylamino)ethyl methacrylate (DMA, 99%, Acros) were vacuum-distilled over CaH_2 . 3-Azidopropyl methacrylate (AzPMA) was prepared by the esterification reaction of 3-azidopropanol and methacryloyl chloride according to literature procedures.³⁶ All purified monomers were stored at $-20\text{ }^\circ\text{C}$ prior to use. Tris(2-(dimethylamino)ethyl)amine (Me_6TREN) was prepared from tris(2-aminoethyl)amine (96%, Acros) following literature procedures.⁴¹ Tetrahydrofuran (THF), methylene chloride (CH_2Cl_2), isopropyl alcohol (IPA), and *N,N*-dimethylformamide (DMF) were distilled just prior to use. *N,N*-Dicyclohexylcarbodiimide (DCC), 4-(dimethylamino)pyridine (DMAP), 2-propanol, ethyl 2-bromoisobutyrate (EBIB, 99%, Avocado), copper(I) chloride (CuCl , 99.995+, Aldrich), copper(I) bromide (CuBr , 99.999%, Aldrich), *N,N,N',N'*-pentamethyldiethylenetriamine (PMDETA, 99%, Aldrich), propargyl ether (99%, Aldrich), and all other reagents were commercially available and used without further purification.

Sample Preparation. *Preparation of Propargyl 2-Chloropropionate (PCP).* The ATRP initiator, PCP, was prepared by the esterification reaction of propargyl alcohol with 2-chloropropionic acid in the presence of DCC and DMAP. A 250 mL round-bottom flask was charged with 2-chloropropionic acid (10.85 g, 0.10 mol), DCC (22.70 g, 0.11 mol), and CH_2Cl_2 (120 mL). The reaction mixture was cooled to $0\text{ }^\circ\text{C}$ in an ice–water bath, and a solution of propargyl alcohol (5.61 g, 0.10 mol), DMAP (0.5 g), and CH_2Cl_2 (30 mL) was added dropwise over a period of 1 h under magnetic stirring. After the addition was completed, the reaction mixture was stirred at $0\text{ }^\circ\text{C}$ for 1 h and then at room temperature for 12 h. After removing the insoluble *N,N*-dicyclohexylurea by suction filtration, the filtrate was concentrated and then was further purified by silica gel column chromatography using CH_2Cl_2 as the

Scheme 2. Synthetic Routes Employed for the Preparation of P(QDMA-co-AzPMA)-g-PNIPAM Cationic Graft Ionomer



eluent. After removing the solvents by rotary evaporator, the obtained residues were distilled under reduced pressure. A colorless liquid was obtained with a yield of $\sim 84\%$. $^1\text{H NMR}$ (CDCl_3 , δ , ppm): 4.76 (2H, $-\text{CH}_2\text{O}-$), 4.43 (H, $-\text{CHCl}-$), 2.51 (H, $-\text{C}\equiv\text{CH}$), and 1.70 (3H, $-\text{CH}_3$).

Synthesis of Monoalkyne-Terminated PNIPAM (Alkyne-PNIPAM).^{42,43} The general procedure employed for the preparation of monoalkyne-terminated PNIPAM was as follows. The mixture containing NIPAM (9.05 g, 80 mmol), Me_6TREN (527 mg, 2.3 mmol), and IPA (18.10 g) was deoxygenated by bubbling with nitrogen for at least 30 min. CuCl (227 mg, 2.3 mmol) was introduced under the protection of N_2 flow. The reaction mixture was stirred for ~ 10 min to allow the formation of $\text{CuCl/Me}_6\text{TREN}$ complex. PCP (335 mg, 2.3 mmol) was then added via a microliter syringe to start the polymerization. The reaction was carried out at $25\text{ }^\circ\text{C}$ and allowed to stir under a N_2 atmosphere for 5 h. Polymerization was terminated by the addition of a few drops of saturated CuCl_2 solution in IPA. The mixture was precipitated into an excess of *n*-hexane. The sediments were collected and redissolved in CH_2Cl_2 and then passed through a neutral alumina column using CH_2Cl_2 as the eluent to remove copper catalysts. The collected eluents were concentrated and precipitated into an excess of anhydrous diethyl ether. This purification cycle was repeated for three times. After drying in a vacuum oven overnight at room temperature, white solids were obtained with an overall yield of $\sim 74\%$. The molecular weight and molecular weight distribution of alkyne-PNIPAM homopolymer were determined by GPC using DMF as eluent: $M_n = 3800$, $M_w/M_n = 1.09$. The degree of polymerization (DP) was determined to be 33 by $^1\text{H NMR}$ analysis in CDCl_3 . $^1\text{H NMR}$ (CDCl_3 , δ , ppm): 4.6 (2H, $-\text{CH}_2-\text{C}\equiv\text{CH}$), 4.0 (33H, $-\text{NH}-\text{CH}-$), 5.8–7.0 (33H, $-\text{NH}-$), and 1.1 (197H, $-\text{CH}_3$).

ATRP Synthesis of P(*t*BMA-co-AzPMA) Statistical Copolymer (Scheme 1). EBIB (49 mg, 0.25 mmol), PMDETA (43 mg, 0.25 mmol), *t*BMA (4.97 g, 35 mmol), and AzPMA (0.84 g, 5 mmol)

were charged into 20 mL glass ampule containing 6 mL of IPA. The ampule was degassed via two freeze–thaw–pump cycles. After freezing the mixture in liquid N_2 , CuCl (25 mg, 0.25 mmol) was introduced. The ampule was further degassed via two freeze–pump–thaw cycles and flame-sealed under vacuum. It was then immersed into an oil bath thermostated at $30\text{ }^\circ\text{C}$ to start the polymerization. After 10 h, the ampule was broken and the viscous reaction mixture was exposed to air. After diluting with CH_2Cl_2 , the solution was precipitated into an excess of $\text{MeOH/H}_2\text{O}$ (1/1, v/v) mixture. After filtration, the residues were redissolved in CH_2Cl_2 and passed through a mixed column of silica gel and neutral alumina using CH_2Cl_2 as the eluent to remove copper catalysts. The combined eluents were concentrated and precipitated into an excess of $\text{MeOH/H}_2\text{O}$ (1/1, v/v). This purification cycle was repeated two times. After drying overnight in a vacuum oven at room temperature, white solids were obtained with a yield of $\sim 77\%$. The molecular weight and molecular weight distribution of P(*t*BMA-co-AzPMA) statistical copolymer were determined by GPC using DMF as the eluent: $M_n = 13\,700$, $M_w/M_n = 1.10$. The AzPMA content of P(*t*BMA-co-AzPMA) was determined to be 14 mol % by $^1\text{H NMR}$ analysis in CDCl_3 . The overall DP of the obtained statistical copolymer was calculated to be 94 on the basis of GPC and NMR results.

Synthesis of P(*t*BMA-co-AzPMA)-g-PNIPAM Graft Copolymer via Click Chemistry (Scheme 1). A mixed solution of P(*t*BMA-co-AzPMA) (1.0 g, 0.96 mmol azido moieties, 1.0 equiv) and alkyne-PNIPAM (1.08 g, 0.28 mmol, 0.29 equiv) in 12 mL of DMF was degassed via two freeze–thaw–pump cycles. CuBr (40 mg, 0.28 mmol, 0.29 equiv) was introduced into the glass ampule under a N_2 atmosphere. After stirring for 24 h at $30\text{ }^\circ\text{C}$, the reaction mixture was exposed to air. After removing all the solvents under reduced pressure, the residues were dissolved in CH_2Cl_2 and precipitated into an excess of *n*-hexane. The sediments were collected and redissolved in CH_2Cl_2 and then passed through a neutral alumina column using CH_2Cl_2 as the eluent to remove copper catalysts. The

combined eluents were concentrated using a rotary evaporator and precipitated into an excess of *n*-hexane. This purification cycle was repeated three times. After drying overnight in a vacuum oven at room temperature, slightly yellowish solids were obtained with a yield of ~95%. The molecular weight and molecular weight distribution of P(*t*BMA-*co*-AzPMA)-*g*-PNIPAM were determined by GPC using DMF as the eluent: $M_n = 34,200$, $M_w/M_n = 1.21$. The NIPAM content in P(*t*BMA-*co*-AzPMA)-*g*-PNIPAM was determined to be 57 mol % by ^1H NMR analysis in CDCl_3 . On average, there are ~3.8 PNIPAM chains per graft copolymer chain.

Selective Hydrolysis of P(*t*BMA-*co*-AzPMA)-*g*-PNIPAM Graft Copolymer (Scheme 1). Into a solution of P(*t*BMA-*co*-AzPMA)-*g*-PNIPAM (1.0 g, 2.8 mmol *t*BMA residues) in 10 mL of CH_2Cl_2 was slowly added TFA (1.0 mL, 13.5 mmol) at 0 °C under vigorous stirring. The reaction mixture was allowed to stir at 0 °C for 3 h and then at room temperature for 8 h. During hydrolysis, the crude products progressively precipitated out. After removing all the solvents under reduced pressure, the residues were dissolved in alkaline solution (pH 9) and dialyzed (MW cutoff, 7000 Da) against deionized water to remove the possible presence of unreacted alkyne-PNIPAM in the previous "click" grafting reaction. After acidification, the anionic graft ionomer, P(MAA-*co*-AzPMA)-*g*-PNIPAM, was obtained as white powders (0.71 g) by freeze-drying and subsequent drying in a vacuum oven at room temperature for 12 h.

ATRP Synthesis of P(DMA-*co*-AzPMA) Statistical Copolymer. EBIB (50 mg, 0.26 mmol), PMDETA (44 mg, 0.26 mmol), DMA (5.50 g, 35 mmol), and AzPMA (0.85 g, 5 mmol) were charged into a 20 mL reaction flask containing 6 mL of IPA. The flask was degassed via three freeze-thaw-pump cycles and backfilled with N_2 . After thermostated at 30 °C, CuCl (26 mg, 0.26 mmol) was then introduced into the reaction flask under protection of N_2 flow to start the polymerization. After 5 h, the resulting viscous reaction mixture was exposed to air and diluted with CH_2Cl_2 . After passing through a neutral alumina column using CH_2Cl_2 as the eluent to remove the copper catalysts and precipitation into an excess of *n*-hexane, the obtained white solids (~79% yield) were dried overnight in a vacuum oven at room temperature. The molecular weight and molecular weight distribution of P(DMA-*co*-AzPMA) statistical copolymer were determined by GPC using DMF as eluent: $M_n = 30\,200$, $M_w/M_n = 1.12$. The AzPMA content of P(DMA-*co*-AzPMA) was determined to be 12 mol % by ^1H NMR analysis in CDCl_3 , and the overall DP of P(DMA-*co*-AzPMA) was calculated to be 190.

Synthesis of P(DMA-*co*-AzPMA)-*g*-PNIPAM Graft Copolymer via Click Chemistry. A solution of P(DMA-*co*-AzPMA) (1.0 g, 0.76 mmol of $-\text{N}_3$ moieties, 1.0 equiv) and alkyne-PNIPAM (0.75 g, 0.19 mmol, 0.25 equiv) in 12 mL of DMF was degassed via two freeze-thaw-pump cycles. CuBr (27 mg, 0.19 mmol, 0.25 equiv) was then introduced into the reaction flask to start the "click" grafting reaction at 30 °C under a N_2 atmosphere. After stirring for 24 h, the reaction mixture was exposed to air. After removing all the solvents under reduced pressure, the obtained polymer was dissolved in CH_2Cl_2 and precipitated into an excess of *n*-hexane. The sediments were redissolved in CH_2Cl_2 and then passed through a neutral alumina column using CH_2Cl_2 as the eluent to remove copper catalysts. The combined eluents were concentrated and precipitated into an excess of *n*-hexane. This purification cycle was repeated three times. After drying in a vacuum oven overnight at room temperature, white solids were obtained with a yield of ~95%. The molecular weight and molecular weight distribution of P(DMA-*co*-AzPMA)-*g*-PNIPAM graft copolymer were determined by GPC using DMF as eluent: $M_n = 56\,400$, $M_w/M_n = 1.19$. The NIPAM content of P(DMA-*co*-AzPMA)-*g*-PNIPAM was determined to be ~50 mol % by ^1H NMR analysis in CDCl_3 . On average, there are ~5.8 grafted PNIPAM chains per graft copolymer chain.

Quaternization of P(DMA-*co*-AzPMA)-*g*-PNIPAM Graft Copolymer. The quaternization of DMA residues was carried out at room temperature by reacting methyl iodide (150 μL , 2.4 mmol) with P(DMA-*co*-AzPMA)-*g*-PNIPAM (0.5 g, 1.6 mmol DMA residues) in THF (35 mL). The reaction was allowed to stir for 1

h at 20 °C. The precipitated residues were collected and thoroughly washed with THF to remove unreacted methyl iodide. It was dissolved in water and thoroughly dialyzed against deionized water (MW cutoff, 7000 Da) to remove impurities and any unreacted alkyne-PNIPAM. After lyophilization, the cationic graft ionomer, P(QDMA-*co*-AzPMA)-*g*-PNIPAM, was obtained as white powders with a yield of 95% after drying overnight in a vacuum oven.

Preparation of Polyion Complex (PIC) Micelles. Predetermined amounts of P(MAA-*co*-AzPMA)-*g*-PNIPAM and P(QDMA-*co*-AzPMA)-*g*-PNIPAM were separately dissolved in water at a concentration of 1.0 g/L; the solution pH was adjusted to 8.0 with aqueous NaOH solution. After filtration through a 0.4 μm Millipore nylon filter, PIC micelles were prepared by mixing these two solutions at varying molar ratios of MAA to QDMA residues, [MAA]:[QDMA]. The molecular weights of the two target polyions were calculated on the basis of M_n values of statistical polymers determined by DMF-GPC analysis and grafted PNIPAM contents determined by ^1H NMR analysis. A bluish tinge was typically observed, indicating the formation of micellar aggregates. The aqueous dispersion of PIC micelles were equilibrated overnight at room temperature before subsequent "click" cross-linking or characterization.

"Click" Core Cross-Linking of PIC Micelles. To 1.0 g/L degassed aqueous solution of the above-prepared PIC micelles at a [MAA]:[QDMA] of 1:1 (200.0 mL, containing 58 μmol of $-\text{N}_3$ moieties), $\text{CuSO}_4 \cdot 5\text{H}_2\text{O}$ (15 mg, 60 μmol), propargyl ether (3 μL , 30 μmol), and sodium ascorbate (11 mg, 60 μmol) were charged.⁴⁴ The molar ratio of propargyl ether to that of total AzPAM residues was kept constant at 1:2. The reaction mixture was stirred at 25 °C for 48 h and then dialyzed (MW cutoff, 14 000 Da) against deionized water for 2 days to remove copper catalysts. The final dispersion exhibits a bluish tinge characteristic of micellar aggregates even in the presence of 1.0 M NaCl, indicating successful "click" core cross-linking reaction.

Characterization. Gel Permeation Chromatography (GPC). Molecular weights and molecular weight distributions were determined by gel permeation chromatography (GPC) equipped with a Waters 1515 pump and a Waters 2414 differential refractive index detector (set at 30 °C). It used a series of three linear Styragel columns HT2, HT4, and HT5 at an oven temperature of 50 °C. The eluent was DMF at a flow rate of 1.0 mL/min. A series of low-polydispersity PMMA standards were employed for the GPC calibration.

Nuclear Magnetic Resonance (NMR) Spectroscopy. All ^1H NMR spectra were recorded in D_2O , CDCl_3 , or DMSO using a Bruker 300 MHz spectrometer. The optical transmittance of the aqueous solution of non-cross-linked and core cross-linked PIC micelles was acquired on a Unico UV/vis 2802PCS spectrophotometer and measured at a wavelength of 500 nm using a thermostatically controlled cuvette. Fourier transform infrared (FT-IR) spectra were recorded on a Bruker VECTOR-22 IR spectrometer. The spectra were collected over 64 scans with a spectral resolution of 4 cm^{-1} .

Laser Light Scattering (LLS). A commercial spectrometer (ALV/DLS/SLS-5022F) equipped with a multitaum digital time correlator (ALV5000) and a cylindrical 22 mW UNIPHASE He-Ne laser ($\lambda_0 = 632$ nm) as the light source was employed for dynamic laser light scattering (LLS) measurements. Scattered light was collected at a fixed angle of 90° for duration of ~10 min. Distribution averages and particle size distributions were computed using cumulants analysis and CONTIN routines. All data were averaged over three measurements.

In static LLS, we can obtain the weight-average molar mass (M_w) and the *z*-average root-mean square radius of gyration ($\langle R_g^2 \rangle^{1/2}$ or written as $\langle R_g \rangle$) of polymer chains in a dilute solution from the angular dependence of the excess absolute scattering intensity, known as Rayleigh ratio $R_{v,v}(q)$, as

$$\frac{KC}{R_{v,v}(q)} \approx \frac{1}{M_w} \left(1 + \frac{1}{3} \langle R_g^2 \rangle q^2 \right) + 2A_2C \quad (1)$$

where $K = 4\pi^2 n^2 (dn/dC)^2 / (N_A \lambda_0^4)$ and $q = (4\pi n / \lambda_0) \sin(\theta/2)$ with N_A , dn/dC , n , and λ_0 being the Avogadro number, the specific refractive index increment, the solvent refractive index, and the wavelength of laser light in a vacuum, respectively, and A_2 is the second virial coefficient. The specific refractive index increment was determined by a precise differential refractometer. Also note that in this study the sample solution was so dilute (0.01 g/L) that the extrapolation of $C \rightarrow 0$ was not necessary, and the term $2A_2C$ in eq 1 can be neglected. Thus, the obtained M_w should be considered as apparent values, denoted as $M_{w,app}$.

Transmission Electron Microscopy (TEM). TEM observations were conducted on a Philips CM 120 electron microscope at an acceleration voltage of 100 kV. Samples for TEM observations were prepared by placing 10 μ L micellar solution at a concentration of 0.1 g/L on copper grids coated with thin films of Formvar and carbon successively. No staining was required.

Results and Discussion

Syntheses of Cationic and Anionic Graft Ionomers. Matyjaszewski et al.³⁶ reported that AzPMA monomer can be polymerized in a controlled manner by ATRP and the obtained PAzPMA can be further derivatized via click reaction with a series of alkynyl-containing small molecules such as propargyl alcohol, propargyl triphenylphosphonium, 4-pentynoic acid, and propargyl 2-bromoisobutyrate. Just recently, they further reported the preparation of molecular brushes by the “click grafting onto” method. Hydroxyl groups of poly(2-hydroxyethyl methacrylate) (PHEMA) were esterified with pentynoic acid; the introduced side alkynyl groups can be further utilized for “click” reactions of monoazide-terminated homopolymers or diblock copolymers, leading to the formation of brush polymers.⁴⁵ However, the grafting efficiency strongly depends on the molecular weights of azide-terminated polymers, which can be up to 88% when PEO- N_3 with an M_n of 775 was employed.

In the current study, general approaches employed for the preparation of graft ionomers bearing oppositely charged backbones and thermoresponsive PNIPAM graft chains, P(MAA-*co*-AzPMA)-*g*-PNIPAM and P(QDMA-*co*-AzPMA)-*g*-PNIPAM, are shown in Schemes 1 and 2, respectively. A three-step approach was employed in both cases. It proceeds first with the synthesis of neutral statistical copolymers of *t*BMA or DMA and azide-containing monomer, followed by grafting alkyne-PNIPAM side chains onto the backbone via “click” chemistry, and the subsequent hydrolysis or quaternization reaction leads to the preparation of target polymers, P(MAA-*co*-AzPMA)-*g*-PNIPAM anionic graft ionomer and P(QDMA-*co*-AzPMA)-*g*-PNIPAM cationic graft ionomer.

Synthesis of P(MAA-*co*-AzPMA)-*g*-PNIPAM Anionic Graft Ionomer (Scheme 1). The statistical copolymer, P(*t*BMA-*co*-AzPMA), was synthesized by ATRP at 30 °C in IPA employing the EBIB/CuCl/PMDETA system. Our trial experiments revealed that this initiator/catalyst system gave better results in terms of monomer conversion and polydispersity of copolymer than those employing 2,2'-bipyridyl or Me₆TREN as the ligands. It has been well-established that the combination of CuCl catalyst and EBIB initiator can allow halogen exchange to occur, thus increasing the relative rate of initiation to propagation and giving a controlled radical polymerization with high initiating efficiency.^{46,47}

As AzPMA monomer and PAzPMA are basically hydrophobic, we intentionally incorporated a relatively low content of AzPMA residues in P(*t*BMA-*co*-AzPMA) to obtain a finally water-soluble P(MAA-*co*-AzPMA)-*g*-PNIPAM graft copolymer, and the feed ratio of *t*BMA to AzPMA monomers was fixed at 7:1. The ¹H NMR spectrum of P(*t*BMA-*co*-AzPMA) in CDCl₃ is shown in Figure 1a, clearly revealing characteristic signals

of *t*BMA residues at $\delta = 1.4$ ppm (*a*) and AzPMA residues at $\delta = 4.0$ (*b*) and 3.4 ppm (*c*). The AzPMA content was then determined to be 14 mol % on the basis of integral ratio of peaks *a* and peaks *b*. DMF GPC trace of the statistical copolymer (Figure 2a) exhibited a monomodal and relatively symmetric peak, reporting a number-average molecular weight, M_n , of 13 700 and a polydispersity, M_w/M_n , of 1.10. On the basis of the above GPC and ¹H NMR results, the overall DP of P(*t*BMA-*co*-AzPMA) was calculated to be 94. Moreover, the FT-IR spectrum of the copolymer (Figure 3a) clearly revealed the presence of an absorbance peak at ~ 2100 cm⁻¹, which is characteristic of azide groups.

The synthesis of alkyne-PNIPAM basically followed similar procedures employed by Stover et al.^{42,43} for the ATRP of NIPAM monomer, with the exception that PCP was used as the ATRP initiator. Grayson et al.⁴⁸ successfully prepared cyclic polystyrene (PS) starting from α -alkyne- ω -bromo heterodifunctional PS synthesized by ATRP using propargyl 2-bromoisobutyrate as the initiator, suggesting that terminal alkynyl moiety does not interfere with the ATRP process. The DMF GPC trace of alkyne-PNIPAM is shown in Figure 2b, revealing a sharp and relatively symmetric peak with an M_n of 3800 and an M_w/M_n of 1.09. No tailing or shoulder at the lower or higher molecular weight side can be discerned, indicating the absence of any premature chain termination, which agrees quite well with the results reported by Stöver et al.^{42,43} The degree of polymerization, DP, of alkyne-PNIPAM was calculated to be 33 by ¹H NMR analysis in CDCl₃.

P(*t*BMA-*co*-AzPMA)-*g*-PNIPAM was synthesized via the “click” grafting of alkyne-PNIPAM onto azide-containing P(*t*BMA-*co*-AzPMA) (Scheme 1). Previous reports have established that click reactions are quite efficient even in the absence of ligands if the solvent can facilitate sufficient solubility for Cu(I) catalysts; thus, the “click” grafting reaction was carried under ligand-free conditions.³⁶ The initial molar ratio of alkynyl residues of alkyne-PNIPAM and azide residues P(*t*BMA-*co*-AzPMA) was designed to be 0.29:1. An excess of azide groups can ensure the complete consumption of alkyne-PNIPAM and further purification is unnecessary. In preliminary steps, we found that if the molar ratio of alkynyl to azide residues is higher than 0.5:1, the presence of unreacted alkyne-PNIPAM can be clearly detected by GPC. Moreover, residual azide groups might be utilized for subsequent “click” cross-linking or further functionalization. The presence of residual azide groups was confirmed by FT-IR results of P(*t*BMA-*co*-AzPMA)-*g*-PNIPAM (Figure 3b). A comparison with the FT-IR spectrum of P(*t*BMA-*co*-AzPMA) (Figure 3a) revealed that the absorbance peak characteristic of azide residues at ~ 2100 cm⁻¹ weakened considerably after “click” grafting reaction.

Figure 1b shows ¹H NMR spectrum of P(*t*BMA-*co*-AzPMA)-*g*-PNIPAM in CDCl₃. Besides signals characteristic of P(*t*BMA-*co*-AzPMA), we can clearly observe characteristic signals of NIPAM residues at $\delta = 5.8$ –7.0 (*f*), 4.0 (*e*), and 1.1 ppm (*d*). On the basis of the integral ratio of peaks *a* and *e*, the molar content of NIPAM residues in P(*t*BMA-*co*-AzPMA)-*g*-PNIPAM was calculated to be 57 mol %, which is in accordance with the target NIPAM content calculated from the feed ratio, indicating a quantitative “click” grafting reaction. On average, there are ~ 3.8 grafted PNIPAM chains per graft copolymer chain.

The GPC trace of P(*t*BMA-*co*-AzPMA)-*g*-PNIPAM using DMF as eluent (Figure 2c) revealed a monomodal elution peak with an M_n of 34 200 and an M_w/M_n of 1.21. The elution peak of the graft copolymer exhibited a clear shift to the higher

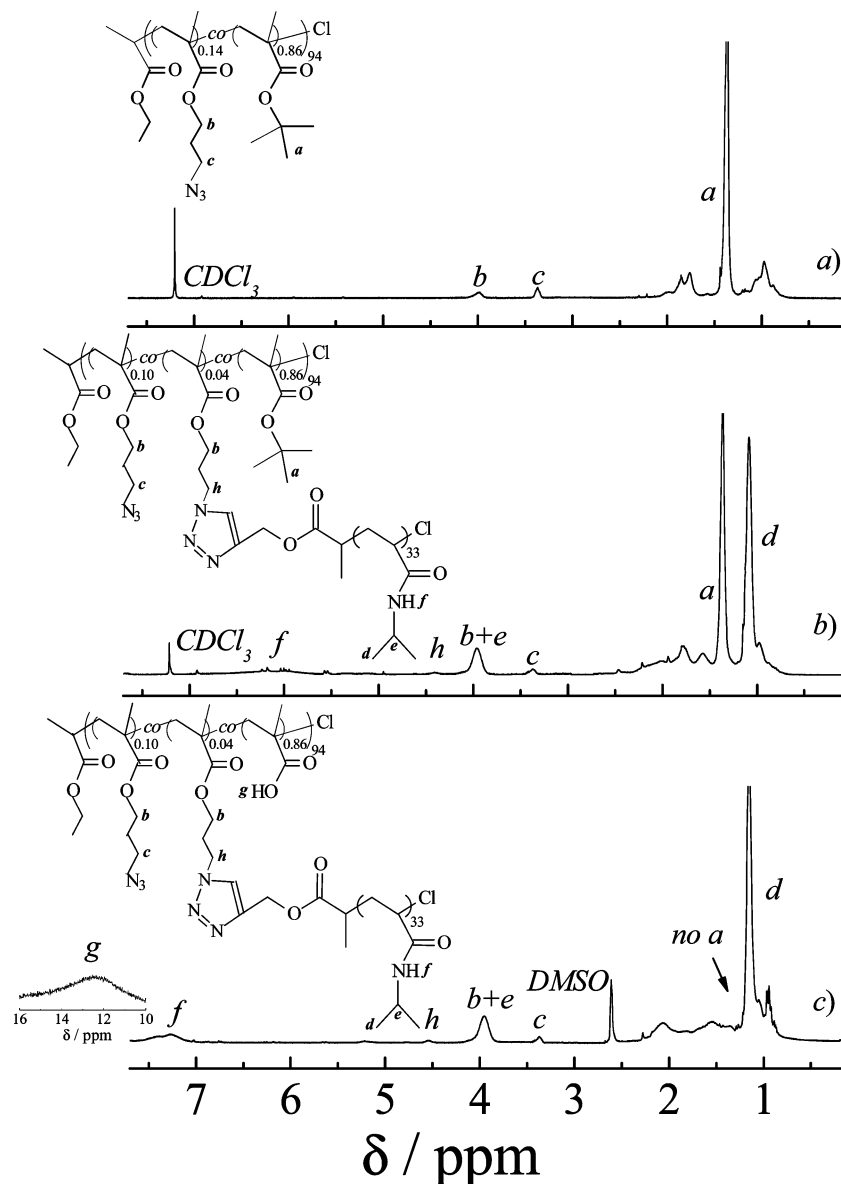


Figure 1. ^1H NMR spectra of (a) P(*t*BMA-*co*-AzPMA) statistical copolymer, (b) P(*t*BMA-*co*-AzPMA)-*g*-PNIPAM graft copolymer in CDCl_3 , and (c) P(MAA-*co*-AzPMA)-*g*-PNIPAM anionic graft ionomer in DMSO obtained via the hydrolysis of P(*t*BMA-*co*-AzPMA)-*g*-PNIPAM in the $\text{CH}_2\text{Cl}_2/\text{TFA}$ mixture.

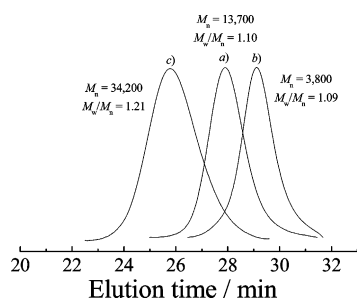


Figure 2. DMF GPC traces of (a) P(*t*BMA-*co*-AzPMA) statistical copolymer, (b) monoalkyne-terminated PNIPAM, and (c) P(*t*BMA-*co*-AzPMA)-*g*-PNIPAM graft copolymer.

molecular weight side; however, it was apparently broader than the two precursors, alkyne-PNIPAM and P(*t*BMA-*co*-AzPMA). The statistical copolymerization of *t*BMA and AzPMA might lead to a distribution of the number of azide residues among different backbone chains. This will lead to the fact that the number of grafted PNIPAM chains may vary considerably from chain to chain.

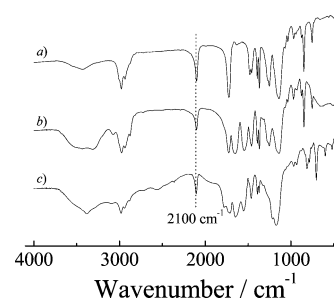


Figure 3. FT-IR spectra of (a) P(*t*BMA-*co*-AzPMA) statistical copolymer, (b) P(*t*BMA-*co*-AzPMA)-*g*-PNIPAM graft copolymer, and (c) P(MAA-*co*-AzPMA)-*g*-PNIPAM anionic graft ionomer.

The target anionic graft ionomer, P(MAA-*co*-AzPMA)-*g*-PNIPAM, was obtained by the hydrolysis of P(*t*BMA-*co*-AzPMA)-*g*-PNIPAM in a $\text{CH}_2\text{Cl}_2/\text{TFA}$ mixture (Scheme 1).⁴⁹ During hydrolysis, the product progressively precipitated out, mainly due to the hydrogen-bonded complexation between PNIPAM side chains and protonated PMAA backbones.^{20,50,51} After removing all the volatile compounds under reduced

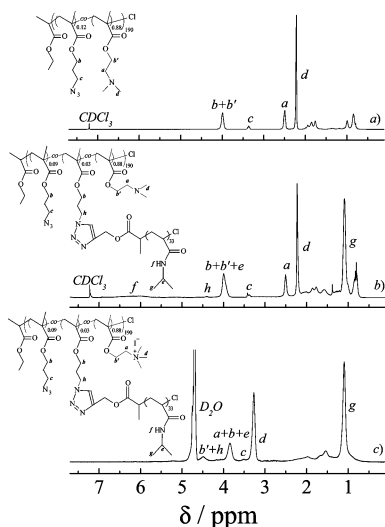


Figure 4. ^1H NMR spectra of (a) P(DMA-*co*-AzPMA) statistical copolymer, (b) P(DMA-*co*-AzPMA)-*g*-PNIPAM graft copolymer in CDCl_3 , and (c) P(QDMA-*co*-AzPMA)-*g*-PNIPAM cationic graft ionomer in D_2O obtained by quaternization of P(DMA-*co*-AzPMA)-*g*-PNIPAM with methyl iodide.

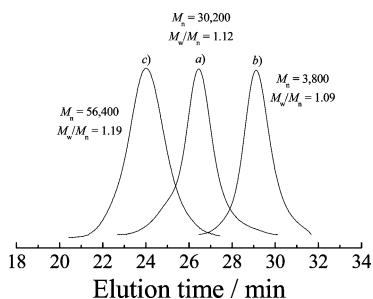


Figure 5. DMF GPC traces of (a) P(DMA-*co*-AzPMA) statistical copolymer, (b) monoalkyne-terminated PNIPAM, and (c) P(DMA-*co*-AzPMA)-*g*-PNIPAM graft copolymer.

pressure, the residues were redissolved in alkaline solution and thoroughly dialyzed against deionized water to remove impurities and any unreacted alkyne-PNIPAM. After acidification, the final product was collected in its protonated form.

The extent of hydrolysis was determined by ^1H NMR in DMSO. The ^1H NMR spectrum (Figure 1c) exhibited the nearly complete disappearance of characteristic signals of *tert*-butyl protons at 1.5 ppm and a new signal of carboxyl protons at $\delta = 11.0$ –14.0 (g), indicating a quantitative removal of *tert*-butyl groups. This can be further confirmed by FT-IR results shown in Figure 3c, revealing the complete disappearance of absorption peak at 1240 cm^{-1} characteristic of C–O–C ether stretching. Most importantly, under the hydrolysis conditions, the residual AzPMA residues were unaffected. This can be clearly confirmed by ^1H NMR (Figure 1c, peak c) and FT-IR spectra (Figure 3c, 2100 cm^{-1}), revealing the presence of residual azide groups after hydrolysis.

Synthesis of P(QDMA-*co*-AzPMA)-*g*-PNIPAM Cationic Graft Ionomer (Scheme 2). The preparation of P(DMA-*co*-AzPMA) followed similar procedures as those described for P(*t*BMA-*co*-AzPMA). Figure 4a shows the ^1H NMR spectrum of P(DMA-*co*-AzPMA) in CDCl_3 , revealing the presence of characteristic DMA and AzPMA residues. AzPMA content was determined to be 12 mol % on the basis of NMR results. DMF GPC trace of P(DMA-*co*-AzPMA) shown in Figure 5a is monomodal and relatively symmetric, revealing an M_n of 30 200 and an M_w/M_n of 1.12. The overall DP of P(DMA-*co*-AzPMA) was calculated to be 190. Moreover, the FT-IR spectrum of

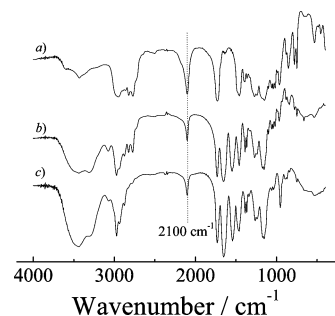


Figure 6. FT-IR spectra of (a) P(DMA-*co*-AzPMA) statistical copolymer, (b) P(DMA-*co*-AzPMA)-*g*-PNIPAM graft copolymer, and (c) P(QDMA-*co*-AzPMA)-*g*-PNIPAM cationic graft ionomer.

P(DMA-*co*-AzPMA) (Figure 6a) clearly revealed the characteristic azide absorbance peak at $\sim 2100\text{ cm}^{-1}$.

The ^1H NMR spectrum in CDCl_3 obtained for P(DMA-*co*-AzPMA)-*g*-PNIPAM after “click” grafting reaction is shown in Figure 4b; we can observe characteristic signals of both precursors. On the basis of the integral ratio of peaks c and e, the NIPAM content in P(DMA-*co*-AzPMA)-*g*-PNIPAM was calculated to be 50 mol %, which agrees quite well with the feed ratio. On average, there are ~ 5.8 grafted PNIPAM chains per graft copolymer chain. The DMF GPC trace in Figure 5b clearly shows a monomodal and symmetric peak without any discernible tailing or shoulder at the lower or higher molecular weight side. The elution peak of the graft copolymer exhibits a considerable shift to the higher molecular weight side compared to the two precursor polymers. The M_n and M_w/M_n values of P(DMA-*co*-AzPMA)-*g*-PNIPAM were determined to be 56 400 and 1.19, respectively.

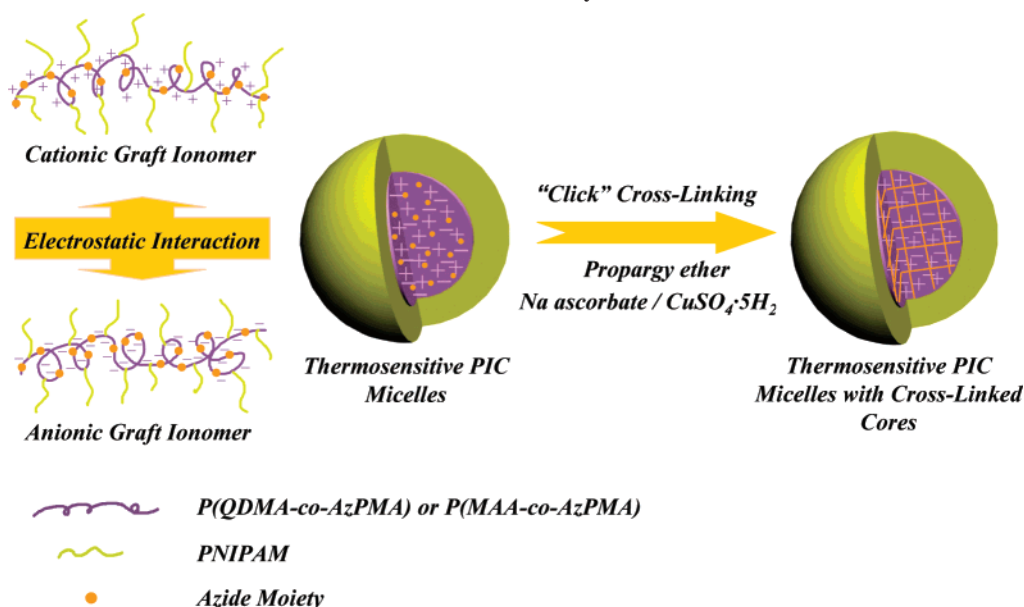
It should be noted that if alkyne-PNIPAM, P(DMAEMA-*co*-AzPMA), and P(DMA-*co*-AzPMA)-*g*-PNIPAM were analyzed by THF GPC, the elution peak of the latter locates within the former two precursors (data not shown). This strongly suggests that in THF GPC analysis polarity differences between polymethacrylate backbones and poly(*N*-isopropylacrylamide) grafts leads to the relatively small or even back shift of the graft copolymer elution peak relative to the precursors. On the other hand, the polarity differences between polymethacrylate backbone and PNIPAM grafts exhibit little effects in GPC analysis using DMF as eluent, which is a much polar solvent than THF.

It should be noted that during the “click” grafting of alkyne-PNIPAM onto the backbones of P(DMA-*co*-AzPMA) (Scheme 2) the molar ratio of alkynyl residues and azide groups was fixed at 1:4. The FT-IR spectrum in Figure 6b revealed that the characteristic azide absorbance peak at $\sim 2100\text{ cm}^{-1}$ weakened to some extent after click reactions.

The target cationic graft ionomer, P(QDMA-*co*-AzPMA)-*g*-PNIPAM, was obtained by the quaternization of P(DMA-*co*-AzPMA)-*g*-PNIPAM with methyl iodide.⁵² This can proceed in a quantitative manner and complete within ~ 1 h. Figure 4c shows the ^1H NMR spectrum of the cationic graft ionomer. Compared to that of P(DMA-*co*-AzPMA)-*g*-PNIPAM, peaks d, a, and b' shifted downfield from 2.3, 2.5, and 4.0 ppm (Figure 4b) to 3.3, 3.9, and 4.6 ppm (Figure 4c), respectively, which indicates that the degree of quaternization is nearly quantitative. It should be noted that the quaternization reaction did not affect AzPMA residues, and the relatively intensity of characteristic azide absorbance peak in the FT-IR spectrum at 2100 cm^{-1} remained unchanged (Figure 6c).

Formation of Polyion Complex (PIC) Micelles. On the basis of above discussions, we successfully synthesized two oppositely

Scheme 3. Schematic Illustration of Formation of Thermosensitive Polyion Complex (PIC) Micelles and Their Core Cross-Linking via Click Chemistry



charged graft ionomers, P(MAA-co-AzPMA)-g-PNIPAM and P(QDMA-co-AzPMA)-g-PNIPAM. It was quite expected that the polyelectrolyte complexation between negatively charged PMAA backbone and positively charged PQDMA backbone will lead to the formation of core-shell nanoparticles consisting of insoluble PIC cores and well-solvated PNIPAM coronas. Moreover, as both graft ionomers contain residual AzPMA residues, the formed PIC micelles can be facily core cross-linked via click chemistry upon addition of a difunctional reagent, propargyl ether (Scheme 3).

PIC micelles were prepared by mixing aqueous solutions of P(MAA-co-AzPMA)-g-PNIPAM and P(QDMA-co-AzPMA)-g-PNIPAM at pH 8.0 and a total concentration of 1.0 g/L, ensuring that MAA residues are completely ionized to bear negative charges on the backbone of graft ionomer.¹⁴ Figure 7 shows dynamic LLS results of PIC micelles prepared at varying [MAA]/[QDMA] molar ratios. Apparently, aqueous solution of PIC micelles formed at [MAA]:[QDMA] = 1:1 exhibits the strongest characteristic bluish scattering tinge. We can clearly tell from Figure 7 that in the [MAA]:[QDMA] range of 1:2 to 2:1 the intensity-average hydrodynamic radii, $\langle R_h \rangle$, are ca. 20–30 nm, exhibiting a minimum value of 21 nm and a relatively narrow size polydispersity (μ_2/Γ^2) of 0.10 at [MAA]:[QDMA] = 1:1. On the other hand, scattered light intensity also exhibits a maximum at [MAA]:[QDMA] = 1:1, indicating that the

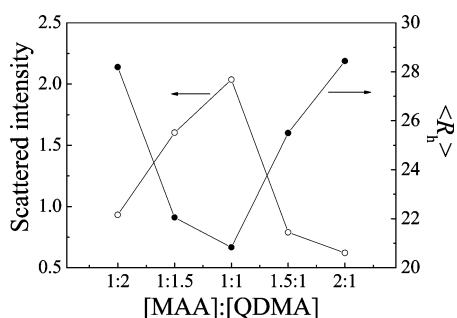


Figure 7. Variation of scattered light intensity and intensity-average hydrodynamic radius, $\langle R_h \rangle$, as a function of mixing molar ratio of MAA to QDMA residues, [MAA]:[QDMA], obtained for 1.0 g/L aqueous solution of PIC micelles (pH 8.0) prepared from P(MAA-co-AzPMA)-g-PNIPAM and P(QDMA-co-AzPMA)-g-PNIPAM.

polyelectrolyte complexation between oppositely charged PMAA and PQDMA backbones proceeds stoichiometrically. Figure 8a shows the TEM image of PIC micelles prepared from these two graft ionomers at [MAA]:[QDMA] = 1:1, which clearly reveals the presence of spherical nanoparticles with diameters in the range of 15–25 nm.

Stuart et al.⁵³ have concluded that PIC micelles only exist in a small window with respect to mixing ratios of the two components and the most compact PIC micelles with the highest aggregation number only form at the mixing ratio where the excess charge of polyelectrolyte mixture is close to zero. This also proves to be true for the current case, in which PIC micellar solution exhibits the largest scattered light intensity and the smallest size at [MAA]:[QDMA] = 1:1. Beyond the [MAA]:[QDMA] range of 1:2 to 2:1, the mixed solutions are optically clear and exhibit very low scattered intensity, suggesting the formation of soluble complexes with quite loose structures.

At a total concentration of 1.0 g/L and [MAA]:[QDMA] = 1:1, azide concentrations originating from P(MAA-co-AzPMA)-g-PNIPAM and P(QDMA-co-AzPMA)-g-PNIPAM are 1.52 and 1.38 μ M, respectively. Deviating from the mixing molar ratio of [MAA]:[QDMA] = 1:1, the unequal azide concentrations of two-component polymers will render the interchain core cross-linking more difficult. Thus, in subsequent studies, we concentrate on PIC micelles prepared at a fixed stoichiometric mixing ratio of [MAA]:[QDMA] = 1:1.

PNIPAM is well-known to be a thermoresponsive polymer that exhibits a lower critical solution temperature (LCST) at ca. 32 °C in aqueous solution.^{54,55} The coronas of PIC micelles consist of PNIPAM chains; thus, we expect this novel type of PIC micelles should also possess thermoresponsiveness (Scheme 3). The temperature dependence of optical transmittance obtained for 0.5 g/L aqueous solution (pH 8.0) of PIC micelles at [MAA]:[QDMA] = 1:1 is shown in Figure 9. At 25 °C the solution exhibits a bluish tinge characteristic of colloidal aggregates of several tens of nanometers. The optical transmittance starts to decrease considerably at 35 °C, indicating that PNIPAM corona is getting water-insoluble due to its thermal phase transition. The transmittance decreases abruptly from 80% at 35 °C to ca. 4% at 45 °C, suggesting extensive thermoinduced aggregation and macroscopic phase separation.

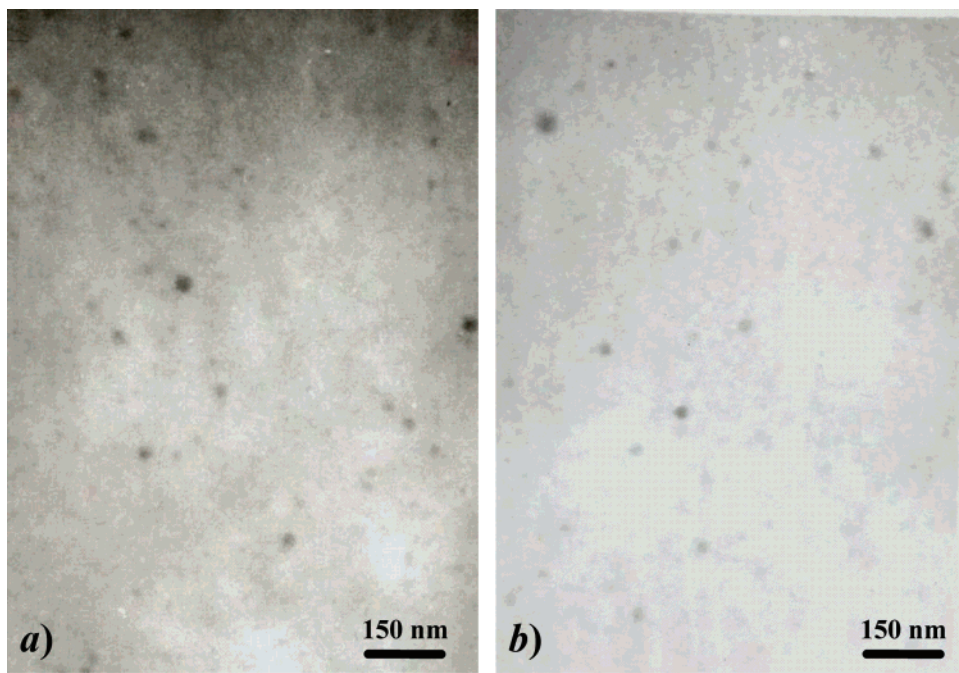


Figure 8. Typical TEM images of (a) non-cross-linked and (b) "click" core cross-linked PIC micelles prepared from P(MAA-*co*-AzPMA)-*g*-PNIPAM and P(QDMA-*co*-AzPMA)-*g*-PNIPAM at [MAA]:[QDMA] = 1:1.

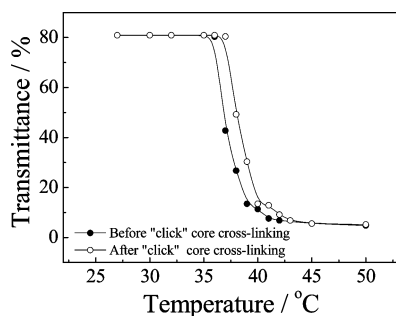


Figure 9. Temperature dependence of optical transmittance at 500 nm obtained for 0.5 g/L aqueous solution (pH 8.0) of (●) non-cross-linked and (○) core cross-linked PIC micelles prepared from P(MAA-*co*-AzPMA)-*g*-PNIPAM and P(QDMA-*co*-AzPMA)-*g*-PNIPAM at [MAA]:[QDMA] = 1:1.

Upon lowering solution pH to 1.4, much stronger scattering can be apparently observed, suggesting the formation of larger aggregates. Figure 10a shows typical hydrodynamic radius distributions, $f(R_h)$, obtained for 0.5 g/L aqueous solutions of PIC micelles. We can observe a bimodal distribution of R_h with two peaks located at ~ 15 and 115 nm. The negatively charged PMAA backbone of P(MAA-*co*-AzPMA)-*g*-PNIPAM at pH 8.0 will be protonated when the solution pH drops below the pK_a of PMAA (~ 5.5).⁵⁶ Thus, lowering solution pH will disintegrate PIC complex micelles due to the disappearance of electrostatic interactions between oppositely charged PMAA and PQDMA backbones. However, hydrogen-bonding interactions between protonated PMAA and PNIPAM side chains will lead to the formation of another type of interpolymer.

On the other hand, the addition of salt will considerably screen electrostatic interactions between oppositely charged backbones. In the presence of 1.0 M NaCl (pH 8.0), the aqueous solution is apparently clear, suggesting the disintegration of PIC micelles. Dynamic LLS reveals a bimodal R_h distribution (Figure 10a). The distribution peak with smaller radius (~ 10 nm) should be ascribed to unimer chains dissociated from PIC micelles. The presence of large aggregates with an average size of ~ 120 nm in radius should be ascribed to the incomplete dissociation

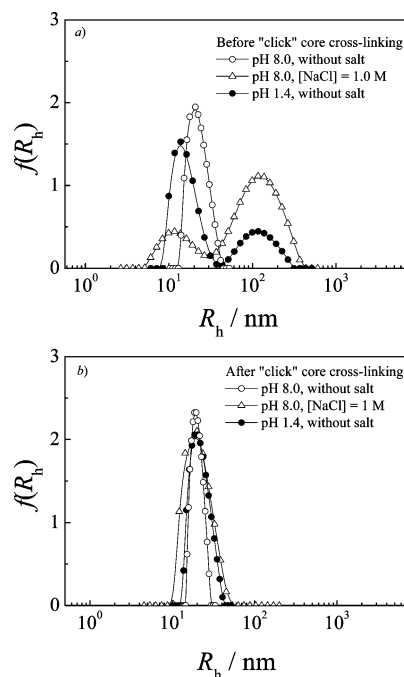


Figure 10. Typical hydrodynamic radius distributions, $f(R_h)$, under different solution conditions obtained for 0.5 g/L aqueous solution (25 °C) of (a) non-cross-linked and (b) "click" core cross-linked PIC micelles prepared from P(MAA-*co*-AzPMA)-*g*-PNIPAM and P(QDMA-*co*-AzPMA)-*g*-PNIPAM at [MAA]:[QDMA] = 1:1.

polyelectrolyte complexes; however, we expect that the large aggregates should possess a quite loose structure.

"Click" Core Cross-Linking of PIC Micelles. PIC micelles formed from P(MAA-*co*-AzPMA)-*g*-PNIPAM and P(QDMA-*co*-AzPMA)-*g*-PNIPAM are unstable upon alterations of solution pH and addition of salts. As both of the component polymers possess residual azide groups, we further explored the core cross-linking of PIC micelles via click reactions in the presence of a difunctional agent, propargyl ether (Scheme 3).

As propargyl ether is hydrophobic, it will be solubilized into the hydrophobic PIC micelle cores upon addition. The molar

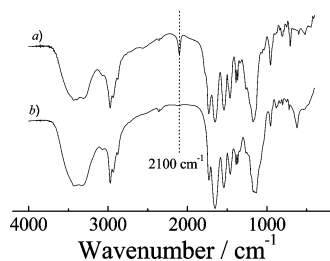


Figure 11. FT-IR spectra of thermosensitive (a) non-cross-linked and (b) “click” core cross-linked PIC micelles prepared from P(MAA-co-AzPMA)-g-PNIPAM and P(QDMA-co-AzPMA)-g-PNIPAM at [MAA]:[QDMA] = 1:1.

ratio of propargyl ether to that of total residual azide groups was kept constant at 1:2, targeting for a theoretical degree of cross-linking of 100%. FT-IR spectra of non-cross-linked and core cross-linked PIC micelles after freeze drying are shown in Figure 11. We can clearly see that the absorbance peak characteristic of azide groups at $\sim 2100\text{ cm}^{-1}$ almost completely disappears. This indicates extensive click reaction between azido and alkynyl moieties, which must lead to the formation of core cross-linked PIC micelles. The successful core cross-linking can be apparently confirmed by the fact that “click” reacted PIC micelles possess the bluish scattering tinge even in the presence of 1.0 M NaCl or lowering the solution pH to < 2 .

Typical hydrodynamic radius distributions, $f(R_h)$, obtained for 0.5 g/L aqueous solution of “click” cross-linked PIC micelles (prepared at [MAA]:[QDMA] = 1:1) under different solution conditions are shown in Figure 10b. The core cross-linked micelles exhibited a $\langle R_h \rangle$ of 19 nm at pH 8.0, which is slightly smaller than that of the PIC micelles before “click” cross-linking (21 nm). This was reasonable considering that the micelle core might contract a little bit upon “click” cross-linking. Static LLS revealed an apparent weight-average molar mass, $M_{w,app}$, of 3.1×10^6 g/mol and an average radius of gyration, $\langle R_g \rangle$, of 17 nm for the “click” cross-linked PIC micelles. Thus, the core cross-linked PIC micelles possessed an average density of $\sim 0.18\text{ g/cm}^3$. If we assume that all oppositely charged graft ionomer chains participated in the formation of PIC micelles, we can then calculate that there were 51 P(MAA-co-AzPMA)-g-PNIPAM chains and 25 P(QDMA-co-AzPMA)-g-PNIPAM chains within one cross-linked PIC micelles. As PNIPAM chains were respectively grafted onto oppositely charged polyelectrolyte backbones, we can speculate that some PNIPAM grafts might be buried within the PIC cores. Thus, the schematic drawing of PIC micelles in Scheme 3 can only be viewed as a simplified cartoon.

Figure 9b shows the temperature-dependent optical transmittance obtained for 0.5 g/L aqueous solution of core cross-linked PIC micelles. Similar to that of non-cross-linked ones, which exhibits a critical aggregation temperature of $\sim 35\text{ }^\circ\text{C}$, the transmittance of the aqueous solution of cross-linked PIC micelles exhibits a critical temperature of $\sim 36\text{ }^\circ\text{C}$, which should be due to the thermal phase transitions of PNIPAM coronas.⁵⁷ Moreover, TEM image of core cross-linked PIC micelles (Figure 8b) revealed the presence of spherical particles, the sizes of which were comparable to that before “click” core cross-linking (Figure 8a).

Upon lowering solution pH to 1.4 or in the presence of 1.0 M salt, dynamic LLS analyses of cross-linked PIC micelles revealed monomodal hydrodynamic radius distribution curves, and the $\langle R_h \rangle$ values were constant at ~ 20 nm (Figure 10b). A closer examination of Figure 10b also told us that size distributions of core cross-linked PIC micelles are slightly

broader at pH 1.4 or in the presence of 1.0 M NaCl. This suggested that in both cases the chain segments within the cross-linked PIC micelles might still rearrange under external pH or salt stimuli. The prominently enhanced structural stability of “click” core cross-linked PIC micelles as compared to non-cross-linked ones strongly suggests that the cross-linking reaction was successful, leading to structurally permanent PIC micelles.

Conclusion

We synthesized two graft ionomers bearing oppositely charged backbones and thermoresponsive PNIPAM side chains. In aqueous solution of their mixtures, PIC micelles consisting of polyelectrolyte complex cores and PNIPAM coronas form due to electrostatic interactions between oppositely charged backbones. As both component copolymer chains bear residual azide residues, we present the first example of structural fixation of PIC micelles via “click” core cross-linking reactions. Compared to non-cross-linked PIC micelles, which are unstable upon lowering solution pH or addition of salts, the “click” cross-linked PIC micelles exhibit much improved structural integrity. Moreover, both the non-cross-linked and cross-linked PIC micelles exhibit thermoinduced dispersion/aggregation in aqueous solution due to the presence of thermosensitive PNIPAM coronas, suggesting that their physical affinity to external substrates can be adjusted with temperature. We expect that this novel type of PIC micelles may offer promising applications as stable nanocarriers for charged compounds or highly efficient nanoreactors of polar compounds in the field of pharmaceutical formulation or biotechnology.

Acknowledgment. This work was financially supported by an Outstanding Youth Fund (50425310) and research grants (20534020 and 20674079) from the National Natural Scientific Foundation of China (NNSFC), the “Bai Ren” Project of the Chinese Academy of Sciences, and the Program for Changjiang Scholars and Innovative Research Team in University (PC-SIRT).

References and Notes

- Colfen, H. *Macromol. Rapid Commun.* **2001**, *22*, 219–252.
- Rodriguez-Hernandez, J.; Lecommandoux, S. *J. Am. Chem. Soc.* **2005**, *127*, 2026–2027.
- Virtanen, J.; Arotcarena, M.; Heise, B.; Ishaya, S.; Laschewsky, A.; Tenhu, H. *Langmuir* **2002**, *18*, 5360–5365.
- Andre, X.; Zhang, M. F.; Muller, A. H. E. *Macromol. Rapid Commun.* **2005**, *26*, 558–563.
- Dai, S.; Ravi, P.; Tam, K. C.; Mao, B. W.; Gang, L. H. *Langmuir* **2003**, *19*, 5175–5177.
- Butun, V.; Liu, S.; Weaver, J. V. M.; Bories-Azeau, X.; Cai, Y.; Armes, S. P. *React. Funct. Polym.* **2006**, *66*, 157–165.
- Poe, G. D.; McCormick, C. L. *J. Polym. Sci., Part A: Polym. Chem.* **2004**, *42*, 2520–2533.
- Gohy, J. F. *Adv. Polym. Sci.* **2005**, *190*, 65–136.
- Riess, G. *Prog. Polym. Sci.* **2003**, *28*, 1107–1170.
- Li, Y.; Lokitz, B. S.; McCormick, C. L. *Angew. Chem., Int. Ed.* **2006**, *45*, 5792–5795.
- Bronstein, L. M.; Sidorov, S. N.; Zhurov, V.; Zhurov, D.; Kabachii, Y. A.; Kochev, S. Y.; Valetsky, P. M.; Stein, B.; Kiseleva, O. I.; Polyakov, S. N.; Shtykova, E. V.; Nikulina, E. V.; Svergun, D. I.; Khokhlov, A. R. *J. Phys. Chem. B* **2005**, *109*, 18786–18798.
- Gohy, J. F.; Varshney, S. K.; Antoun, S.; Jerome, R. *Macromolecules* **2000**, *33*, 9298–9305.
- Hu, Z. J.; Jonas, A. M.; Varshney, S. K.; Gohy, J. F. *J. Am. Chem. Soc.* **2005**, *127*, 6526–6527.
- Harada, A.; Kataoka, K. *Macromolecules* **1995**, *28*, 5294–5299.
- Kabanov, A. V.; Vinogradov, S. V.; Suzdaltseva, Y. G.; Alakhov, V. Y. *Bioconjugate Chem.* **1995**, *6*, 639–643.
- Vinogradov, S.; Batrakova, E.; Li, S.; Kabanov, A. *Bioconjugate Chem.* **1999**, *10*, 851–860.
- Harada, A.; Kataoka, K. *J. Controlled Release* **2001**, *72*, 85–91.
- Harada, A.; Kataoka, K. *Macromolecules* **1998**, *31*, 288–294.

- (19) Nishiyama, N.; Kataoka, K. *Polym. Ther. II* **2006**, *193*, 67–101.
- (20) Liu, S. Y.; Zhu, H.; Zhao, H. Y.; Jiang, M.; Wu, C. *Langmuir* **2000**, *16*, 3712–3717.
- (21) Zhang, W. Q.; Shi, L. Q.; Gao, L. C.; An, Y. L.; Li, G. Y.; Wu, K.; Liu, Z. *Macromolecules* **2005**, *38*, 899–903.
- (22) Kabanov, A. V.; Bronich, T. K.; Kabanov, V. A.; Yu, K.; Eisenberg, A. *Macromolecules* **1996**, *29*, 6797–6802.
- (23) Kakizawa, Y.; Kataoka, K. *Adv. Drug Delivery Rev.* **2002**, *54*, 203–222.
- (24) Jaturanpinyo, M.; Harada, A.; Yuan, X. F.; Kataoka, K. *Bioconjugate Chem.* **2004**, *15*, 344–348.
- (25) Harada, A.; Kataoka, K. *J. Am. Chem. Soc.* **2003**, *125*, 15306–15307.
- (26) Harada, A.; Kataoka, K. *J. Am. Chem. Soc.* **1999**, *121*, 9241–9242.
- (27) Park, J. S.; Akiyama, Y.; Yamasaki, Y.; Kataoka, K. *Langmuir* **2007**, *23*, 138–146.
- (28) Tsolakis, P.; Bokias, G. *Macromolecules* **2006**, *39*, 393–398.
- (29) Kakizawa, Y.; Harada, A.; Kataoka, K. *J. Am. Chem. Soc.* **1999**, *121*, 11247–11248.
- (30) Bontha, S.; Kabanov, A. V.; Bronich, T. K. *J. Controlled Release* **2006**, *114*, 163–174.
- (31) Miyata, K.; Kakizawa, Y.; Nishiyama, N.; Harada, A.; Yamasaki, Y.; Koyama, H.; Kataoka, K. *J. Am. Chem. Soc.* **2004**, *126*, 2355–2361.
- (32) Miyata, K.; Kakizawa, Y.; Nishiyama, N.; Yamasaki, Y.; Watanabe, T.; Kohara, M.; Kataoka, K. *J. Controlled Release* **2005**, *109*, 15–23.
- (33) Yuan, X. F.; Yamasaki, Y.; Harada, A.; Kataoka, K. *Polymer* **2005**, *46*, 7749–7758.
- (34) Hartmuth, C.; Kolb, M. G. F. K. B. S. *Angew. Chem., Int. Ed.* **2001**, *40*, 2004–2021.
- (35) Tsarevsky, N. V.; Sumerlin, B. S.; Matyjaszewski, K. *Macromolecules* **2005**, *38*, 3558–3561.
- (36) Sumerlin, B. S.; Tsarevsky, N. V.; Louche, G.; Lee, R. Y.; Matyjaszewski, K. *Macromolecules* **2005**, *38*, 7540–7545.
- (37) Gondi, S. R.; Vogt, A. P.; Sumerlin, B. S. *Macromolecules* **2007**, *40*, 474–481.
- (38) O'Reilly, R. K.; Joralemon, M. J.; Hawker, C. J.; Wooley, K. L. *Chem.—Eur. J.* **2006**, *12*, 6776–6786.
- (39) O'Reilly, R. K.; Joralemon, M. J.; Hawker, C. J.; Wooley, K. L. *New J. Chem.* **2007**, *31*, 718–724.
- (40) Schild, H. G. *Prog. Polym. Sci.* **1992**, *17*, 163–249.
- (41) Ciampolini, M.; Nardi, N. *Inorg. Chem.* **1966**, *5*, 41–44.
- (42) Xia, Y.; Yin, X.; Burke, N.; Stover, H. *Macromolecules* **2005**, *38*, 5937–5943.
- (43) Xia, Y.; Burke, N.; Stover, H. *Macromolecules* **2006**, *39*, 2275–2283.
- (44) O'Reilly, R. K.; Joralemon, M. J.; Wooley, K. L.; Hawker, C. J. *Chem. Mater.* **2005**, *17*, 5976–5988.
- (45) Gao, H. F.; Matyjaszewski, K. *J. Am. Chem. Soc.* **2007**, *129*, 6633–6639.
- (46) Karanam, S.; Goossens, H.; Klumperman, B.; Lemstra, P. *Macromolecules* **2003**, *36*, 3051–3060.
- (47) Shipp, D. A.; Wang, J. L.; Matyjaszewski, K. *Macromolecules* **1998**, *31*, 8005–8008.
- (48) Laurent, B. A.; Grayson, S. M. *J. Am. Chem. Soc.* **2006**, *128*, 4238–4239.
- (49) Hou, S. J.; Chaikof, E. L.; Taton, D.; Gnanou, Y. *Macromolecules* **2003**, *36*, 3874–3881.
- (50) Chen, G. H.; Hoffman, A. S. *Nature (London)* **1995**, *373*, 49–52.
- (51) Zhang, W. Q.; Shi, L. Q.; Miao, Z. J.; Wu, K.; An, Y. L. *Macromol. Chem. Phys.* **2005**, *206*, 2354–2361.
- (52) Butun, V.; Armes, S. P.; Billingham, N. C. *Macromolecules* **2001**, *34*, 1148–1159.
- (53) van der Burgh, S.; de Keizer, A.; Stuart, M. A. C. *Langmuir* **2004**, *20*, 1073–1084.
- (54) Arotcarena, M.; Heise, B.; Ishaya, S.; Laschewsky, A. *J. Am. Chem. Soc.* **2002**, *124*, 3787–3793.
- (55) Virtanen, J.; Arotcarena, M.; Heise, B.; Ishaya, S.; Laschewsky, A.; Tenhu, H. *Langmuir* **2002**, *18*, 5360–5365.
- (56) Shatayeva, L. K.; Samsonov, G. V.; Vacik, J.; Kopecek, J.; Kalal, J. *J. Appl. Polym. Sci.* **1979**, *23*, 2245–2251.
- (57) Alarcon, C. D. H.; Pennadam, S.; Alexander, C. *Chem. Soc. Rev.* **2005**, *34*, 276–285.

MA702199F